Chapter 5: Spatiotemporal Self-Organization on a Pt Ribbon Electrode

5.1 Introduction

The coupling function in the reaction-migration formalism is strongly influenced by the non-homogeneous current density and double layer potential at the edge of the electrode, when the electrode is embedded in an insulating plane, *e.g.*, disc, ribbon electrode. A lot of studies were carried out with disc electrodes embedded in insulating material. An important result regarding current and potential distributions at disc electrodes, studied by Newman [98, 99], is that because of the ohmic potential drop, a uniform current density and uniform double layer potential cannot coexist. At the edge of a disc electrode, the effective resistance is at a minimum, whereas it is at a maximum at the center. Thus, the current density and double layer potential are always largest at the edge and decrease toward the middle of the electrode. This position-dependent effective resistance leads to strong coupling of every position to edge-near positions of the electrode and to complicated coupling functions which are explicitly position-dependent [34].

Theoretical derivation of the edge effect on a ribbon electrode is similar to that on a disc electrode. The following discussion follows the theory of Christoph [34]. Figure 5.1 shows the distribution of the double layer potential of a thin ribbon electrode. The double layer potential is increasing at both edges of the electrode due to the decreasing effective resistance at the edges. The change of the double layer potential can be simplified for one dimensional double layer dynamics:

$$\partial u_t(x,t) = -i_r(u) + \kappa h(x)(E_0 - u) + \kappa \int_0^1 H_0(x,x')(u(x') - u(x))dx' \qquad (5.1)$$

where both the coupling function $H_0(x, x')$ and the local function $h(x)$ are position-dependent. The coupling function for a thin ribbon electrode decreases as the distance between two coupled electrode points increases and diverges at the edges of electrode.

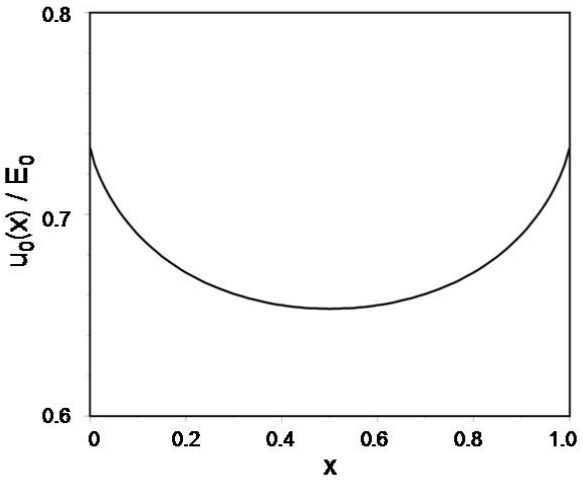

Figure 5.1. Double layer potential distribution on a thin ribbon electrode. Double layer potential is increasing both edges of electrode. After Christoph [34].

Pattern formation in the electrocatalytic oxidation of formic acid on a Pt ribbon electrode is much different from the Pt ring electrode system; pattern formation on the ring strongly depends on the distance between the ring and the reference electrode [21] and whole the surface of the ring electrode is affected equally by the (symmetric) reference electrode. However, the surface of the ribbon electrode is affected unequally by the reference electrode. In addition, edge effects influence the distribution of the interfacial potential. Lee [21] introduced experiments on pattern formation using a Pt ribbon electrode in the electrocatalytic oxidation of formic acid. Because of the geometry effect, in-phase or anti-phase edge oscillations were observed during the current oscillations under positive, negative coupling respectively. The inhomogeneous behavior of the active state is relatively

higher than that of the passive state on a ribbon electrode. The edges of the ribbon tended to be more passive compared to the center. When the distance between the working and reference electrode decreases, negative coupling needed to be taken into account in order to interpret the distribution of the interfacial potential in Figure 5.2.

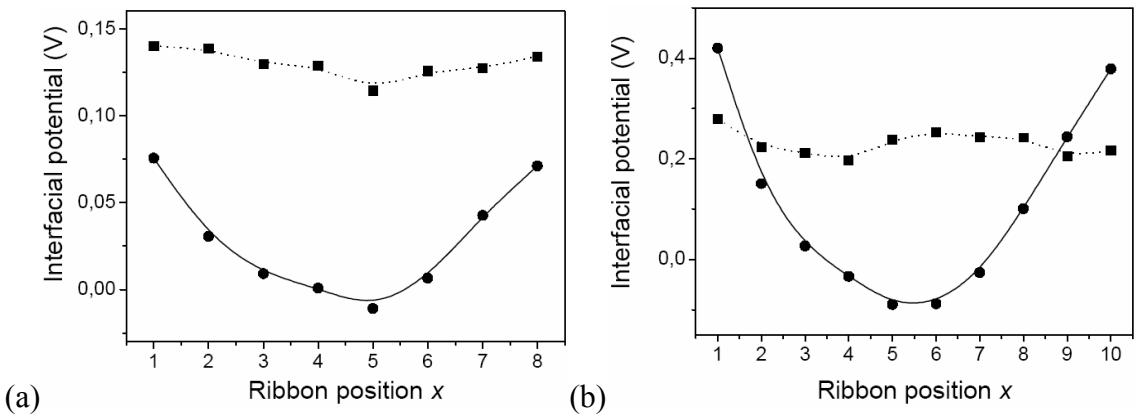

Figure 5.2. Distribution of interfacial potential during bistability on a ribbon electrode due to (a) positive and (b) negative non-local coupling (■: passive state, ●: active state). Due to the negative coupling, the interfacial potential at the edges is higher than that of the passive state. After Lee [21].

In this work, we first reproduced the local inhomogeneity and migration coupling caused by the edge effect of the ribbon electrode. The local interfacial potential was observed by applying a negative potential perturbation in the active state in order to visualize the coupling function. In addition the active transitions during the local/remote triggering from the passive state in the bistable regime were investigated. In addition, the pattern formation, which depends on the position of reference electrode above the ribbon electrode, was described in the oscillatory regime.

5.2 Experimental

The schematic diagram of the principal three-electrode arrangement is shown in Figure 5.3. A smooth polycrystalline Pt ribbon was used as the working electrode (WE). Two Pt coils (thickness of 1 mm wire) used as counter electrode (CE) was placed 80 mm

above the WE. The tip of a Luggin-Haber capillary hosting a Hg/Hg_2SO_4, K_2SO_4 (sat'd) reference electrode (RE) was placed at the symmetrical axis which was the center of the ribbon. In other condition, we changed the position of RE which placed at the asymmetrical axis; near position 1, or between positions 2 and 3 of the ribbon WE. The distance of RE from the WE was β (the distance between WE and RE divided by the length of WE). Pulse electrode (PE) was Pt wire sealed in a glass except for a 2 mm. It was positioned above the WE up to about 1 mm (between positions 2 and 3, center or position 8). In order to measure the instantaneous local interfacial potentials on the Pt ribbon WE, eight potential microprobes were placed along the ribbon electrode close to the electrode surface (0.2 mm). Each microprobe capped with the Hg/Hg_2SO_4 electrode were filled a 0.5M Na_2SO_4 solution (Merck, p.a.).

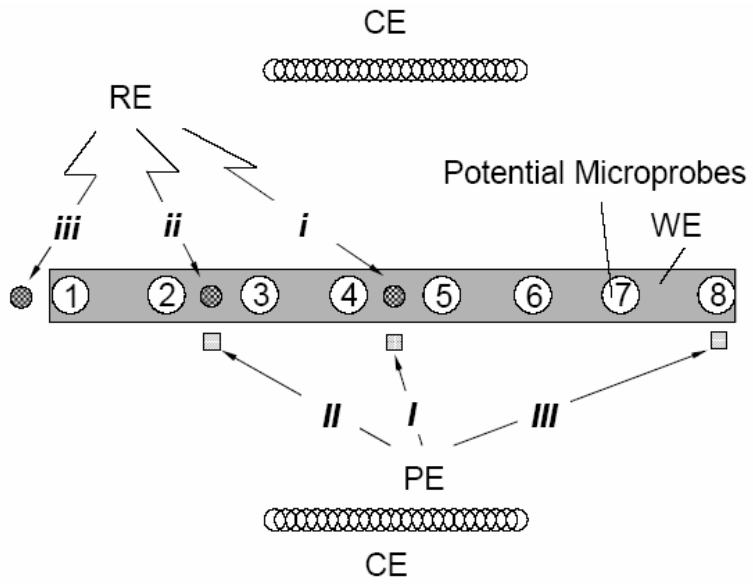

Figure 5.3. Schematic view of the experimental setup of ribbon electrode. The position of RE (i~iii) and PE (I~III) were varied in different experiments as indicated.

All solutions were prepared with ultrapure water (Millipore Milli-Q water, 18 MΩ·cm) and were kept at room temperature. Before each experiment, the Pt ribbon WE was chemically cleaned (as shown in Figure 2.2). For investigation of the electrocatalytic oxidation of formic acid, 0.1 M HCOONa (Merck, p.a.) in 0.033 M H_2SO_4 was used as the electrolyte. We added 1×10^{-6} M bismuth ions into the main solution to make the oscillatory

condition. The electrolyte was extensively bubbled with N_2 before each experiment. A home-built potentiostat (Electronic Laboratory of Fritz-Haber-Institut) was used for all cyclic voltammetry experiments and programmable function generator (HM 8130, HAMEG) providing rectangular potential pulses of various amplitude and duration.

5.3 Experimental results

5.3.1 Potential perturbation in the active state

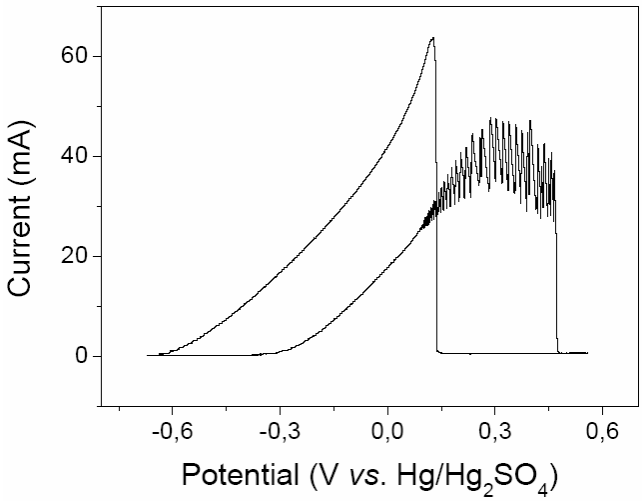

Figure 5.4. Cyclic voltammetry on a Pt ribbon electrode. Scan rate is 10 mV/s and solution is 0.1 M HCOONa / 0.033M H_2SO_4 with 1×10^{-6} M Bi^{3+}. Position of RE (β = 0.17) is at the center of WE (i).

Figure 5.4 displays the current-potential characteristic for the oxidation of formic acid during cyclic voltammetry on a polycrystalline Pt ribbon electrode with a scan rate of 10 mV/s and added bismuth ions. On the anodic scan, the electrode is in the activate state before the broad current oscillatory regime during the oxidation of formic acid. After the oscillatory regime, the electrode is switched to the passive state because of the poisoning of oxygen-containing species on the electrode. On the cathodic scan, the deactivated electrode turns to the active state. These sorts of bistability and oscillations were shown in (H)N-NDR condition of electrochemical system [51].

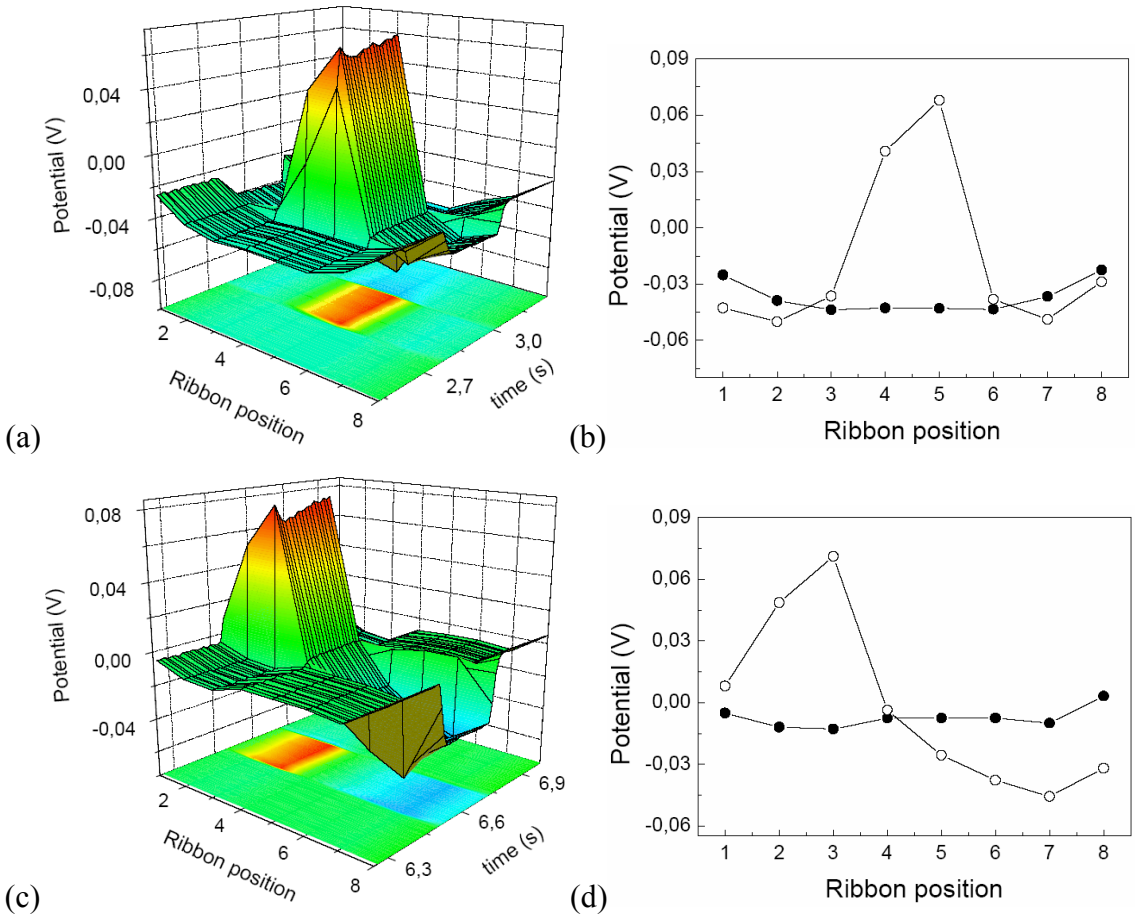

Figure 5.5. (a) Spatiotemporal local potential distribution and (b) instantaneous spatial potential profile, RE (i) and PE (I) were placed at the center of the WE, at U = +0.033 V and U_{pulse} = -5 V (200 ms). (c) Spatiotemporal local potential distribution and (d) instantaneous spatial potential profile, RE (ii) and PE (II) were placed between positions 2 and 3 of the WE, at U = +0.039 V and U_{pulse} = -5 V (200 ms). β is 0.17(●: initial active state, ○: transition state during the application of potential perturbation).

In Figure 5.5 the local response to a negative potential perturbation is displayed in order to visualize the coupling function on a ribbon electrode by subthreshold perturbation at different positions. Local response to a negative potential perturbation (-5 V, 200 ms) is shown in Figure 5.5(a) when the RE was placed the center of the WE (β = 0.17) in active state (+0.033 V) on the anodic scan. The position of pulse electrode was the center of the WE. As a negative potential perturbation was applied, the potential distribution rose at the position of the PE (position 4-5). However the local potential near the two edges

decreased during the perturbation (position 2 and 7), whereas the potential distribution at two edges (position 1 and 8) increased again, in Figure 5.5(b). The local inhomogeneity was observed more clearly in Figure 5.5(c). The RE and PE were placed between positions 2 and 3 of the WE. When applying a negative potential perturbation (-5 V, 200 ms) in the active state (+0.039 V), the interfacial potential rose at the position of the PE (position 2-3) while interfacial potential decreased as getting near to the edge (position 5-6 and 7). But the interfacial potential distribution increased obviously at the edge (position 8) in Figure 5.5(d). Because of the strong potential perturbation, the increasing interfacial potential was not observed clearly at the other edge (position 1). This qualitative analysis is in agreement with theory which was used to rationalize following results (see Figure 5.12).

5.3.2 Front transition on ribbon electrode in the bistable regime (local & remote triggering)

When a positive potential perturbation (+10 V, 20 ms) was applied at one edge of the WE (position 8) in the passive state (+0.19 V) of the bistable regime, the surface of the WE was changed fast to the active state (local triggering). After applying the perturbation, the current increased sharply because the surface of ribbon electrode changed fast to the active state in Figure 5.6(a). In Figure 5.6(b), the speed of the activation front gradually increased after the beginning of the transition and the front had maximum speed in the center of the electrode (position 4). When the activation front passed over the center of the ribbon, the front velocity decreased again

In contrast, when a negative potential perturbation (-10 V, 20 ms) was applied at one edge (position 8) of the ribbon electrode in the passive state (+0.19 V) of the bistable regime, again the current increased (Figure 5.6(c)) and the surface of ribbon electrode changed to the active state. However, an activation front was triggered at the opposite end of the ribbon (position 1), which at first spread very fast, then slowed down continuously until it reached the other dege.

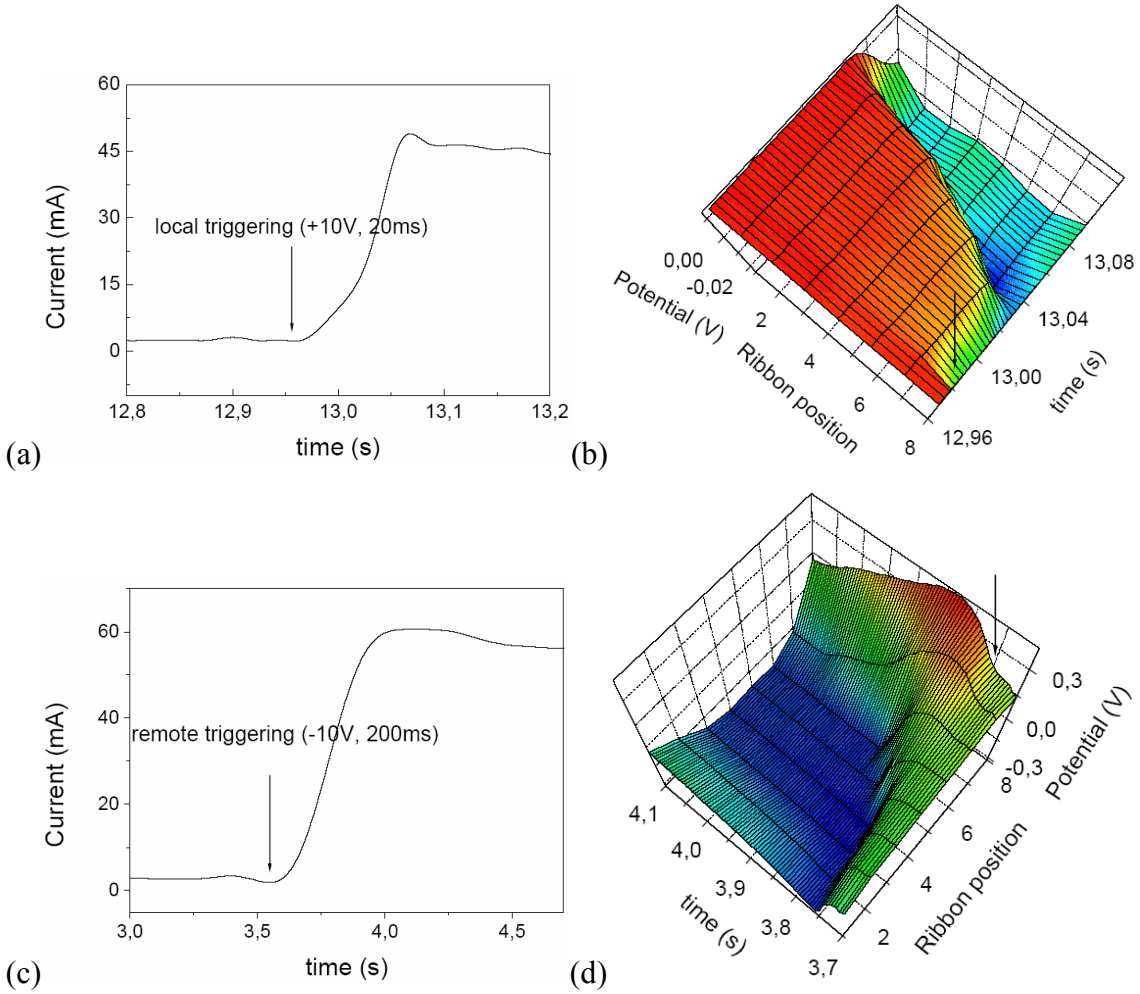

Figure 5.6. (a) Total current and (b) potential distribution during local triggering; U = +0.19 V and U_{pulse} = +10 V (20 ms). (c) Total current and (d) potential distribution during remote triggering; U = +0.19 V and U_{pulse} = -10 V (200 ms). RE (β = 0.17) was placed at the center of WE (i), PE was placed at the edge of WE (III).

5.3.3 Effects of RE position in the oscillatory regime

The spatiotemporal pattern formation of the interfacial potential was observed when the current oscillations occurred during cyclic voltammetry with a scan rate of 1 mV/sec. During period-2 current oscillations in figure 5.7(a), symmetric anti-phase patterns, whose center was the RE position (center of the WE), were observed with small β (β = 0.3). The activation began at one edge, the next activation at the other edge. The position of the

passive state changed from one edge to the other at the same time (Figure 5.7(b)). At higher voltage, current oscillations were period-2 with lower frequency and higher amplitude as shown in Figure 5.7(c).

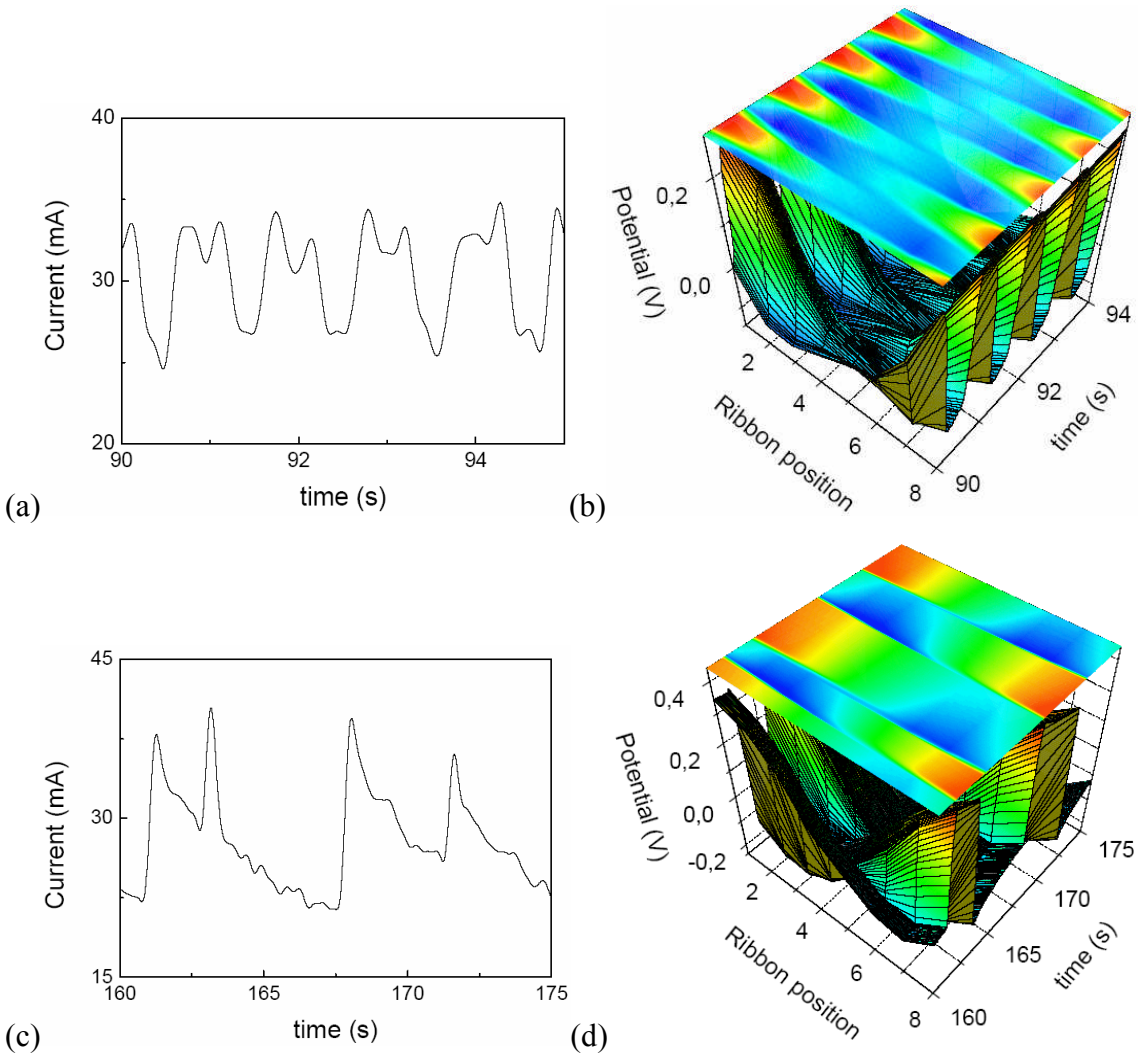

Figure 5.7. During cyclic voltammetry, (a) current oscillations and (b) spatiotemporal pattern formation of the interfacial potential at the beginning of oscillations. At higher voltage (after 160 s) (c) current oscillations and (d) spatiotemporal pattern of the interfacial potential. The RE was placed at the center of the WE (i) with small β (β = 0.3).

When the RE was moved from the center horizontally, asymmetric RE position (between positions 2 and 3) in small β (β = 0.3), we observed different spatiotemporal pattern formation reproduced in Figure 5.8. When the period-2 current oscillations occurred in Figure 5.8(a), asymmetric anti-phase oscillations were observed at both edges in Figure 5.8(b) at the same time. During the current oscillations small active and passive patterns were observed at the edge near the RE, strong ones at the other edge far from the RE. These active and passive patterns had an asymmetric center that was the position of the RE (between positions 2 and 3).

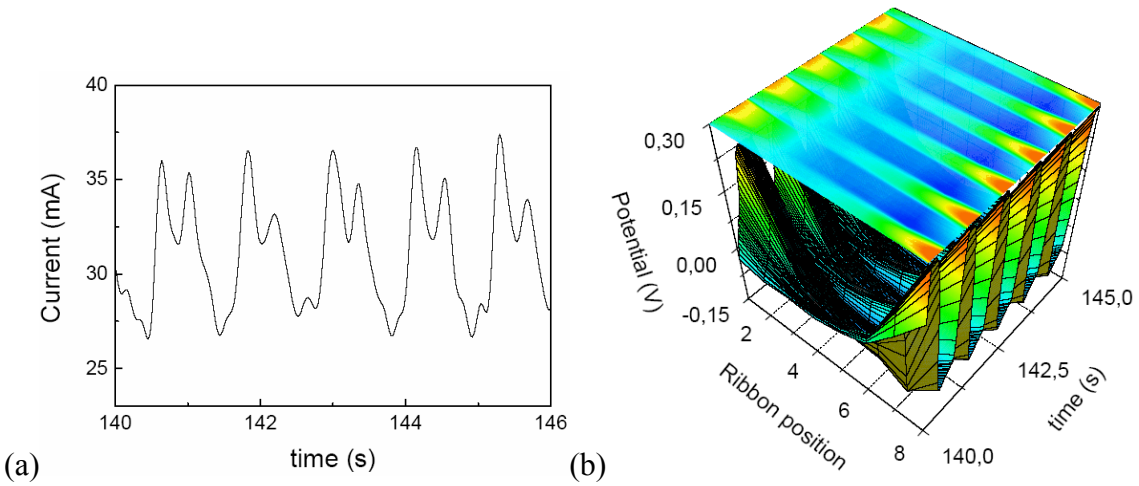

Figure 5.8. During cyclic voltammetry, (a) current oscillations and (b) spatiotemporal pattern formation of interfacial potential. RE was placed between positions 2 and 3 of the WE (ii) (β = 0.3).

When the RE was positioned out of the ribbon electrode (near position 1) with small β (β = 0.3), we observed the spatiotemporal pattern shown in Figure 5.9. Current oscillations and pattern were similar to Figure 5.8. But, during the current oscillations in Figure 5.9(a), the spatiotemporal pattern had different oscillations frequency at both edges, i.e., one side of the electrode (position 1) oscillated with a frequency twice as high as the one at other side of the electrode (position 8) as shown in Figure 5.9(b). A similar theoretical result was shown in ref. [100].

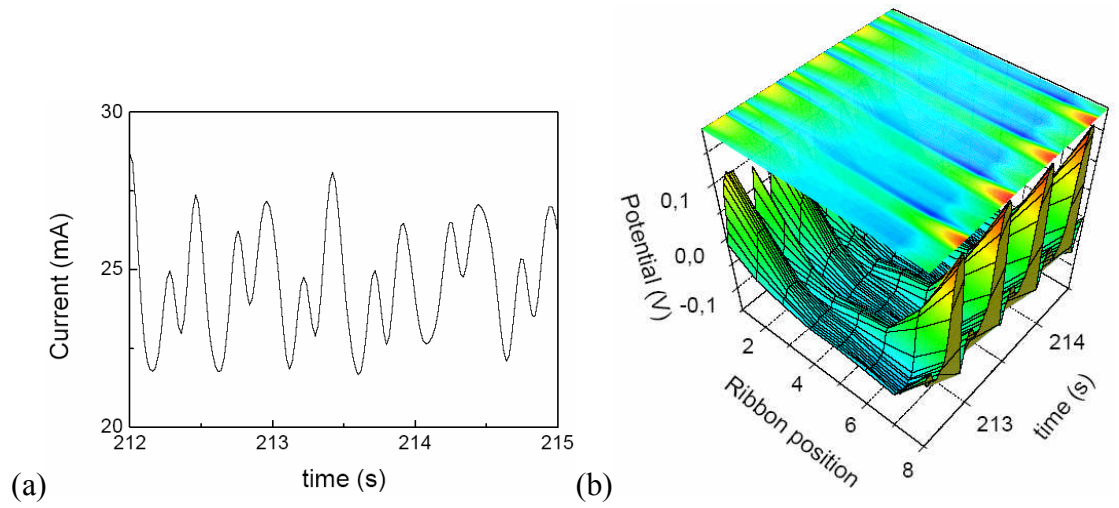

Figure 5.9. During cyclic voltammetry, (a) current oscillations and (b) spatiotemporal pattern formation of interfacial potential. RE was placed at one edge of WE (iii) (β = 0.3).

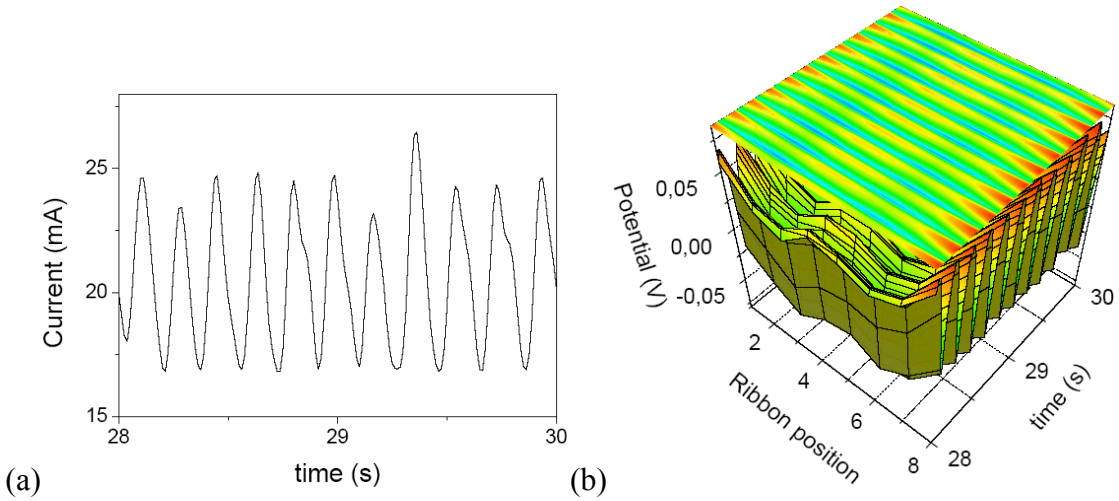

Figure 5.10. During cyclic voltammetry, (a) current oscillations and (b) spatiotemporal pattern formation of interfacial potential. The RE was placed at the center of the WE (i) (β = 0.5).

For large β (β = 0.5) and symmetric position of the RE (center of the WE), period-1 current oscillation occurred in Figure 5.10(a). At the same time, in-phase edge oscillations were observed in Figure 5.10(b) due to the positive coupling.

5.4 Summary and discussion

Coupling functions can and have been derived for a number of electrode geometries [34]. One of the most widely used electrodes is the ribbon electrode embedded in an insulating plane. The main differences compared to the discussed thin ring electrode is the emergence of edge effects which have long been known in electrochemistry and are essentially related to the electrostatic fact that the charge density diverges at the discontinuous gap between electrode and insulating plane. In terms of electrochemistry, this effect manifests itself in a higher current density (caused by a better current transport also from the insulating planes) at the edges of the ribbon compared to the center regions.

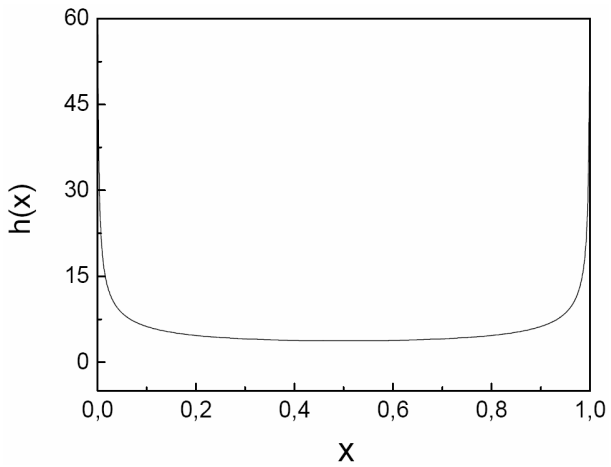

Figure 5.11. Local function $h(x)$ of ribbon electrode in 2-dimensional geometry models. $h(x)$ depends on space. So the resistivity can be considered has a function of space $\rho = \rho(x) = 1/(\kappa h(x))$, therefore the local dynamics as well as the stationary states generally are inhomogeneous [34].

For 2-dimensional geometry models with edges, the local function $h(x)$ is shown in Figure 5.11. The local function along the ribbon has higher values at the two edges compared with other positions. Consequently, the local effective resistance is extremely small at the edges.

Examples of coupling functions $H_0(x, x')$ with different β are reproduced in Figure 5.12. For large β (positive coupling function in Figure 5.12(a)) the coupling strength decreases with distance but rise sharply at the edges. With small β (figure 5.12(b)), the coupling function near the two edges decreases almost to zero, and the strength of coupling increases at the edges again for $x = 0.5$. For $x = 0.25$, the coupling strength is positive near one edge from the RE position, but becomes negative near the other edge, where it therefore diverges to $-\infty$.

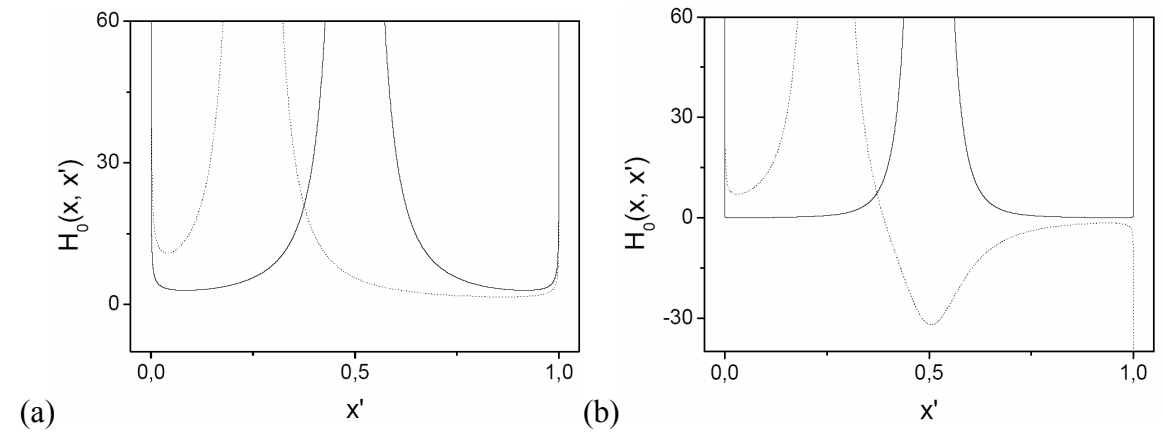

Figure 5.12. (a) Coupling function for $\beta = 100$ and (b) $\beta = 0.1$. In both cases $H_0(x, x')$ is shown for two positions $x = 0.5$ and $x = 0.25$.

The results of front triggering with small β can be easily rationalized in terms of these coupling functions; for local triggering the variations of activation front velocity (maximum near center) are due to the local function $h(x)$, which indicates that the center tends to be more active, and more easily activated. The resulting activation front then slows down approaching the other edge, presumably because of the influence of the local function $h(x)$. A computer simulation of an active front is shown in Figure 5.13, in good agreement with the experimental result (Figure 5.6(b)). For the remote triggering, the negative perturbation affects regions on the other end of the ribbon where $H_0(x, x') < 0$, all these regions activate very rapidly (almost half of the electrode).

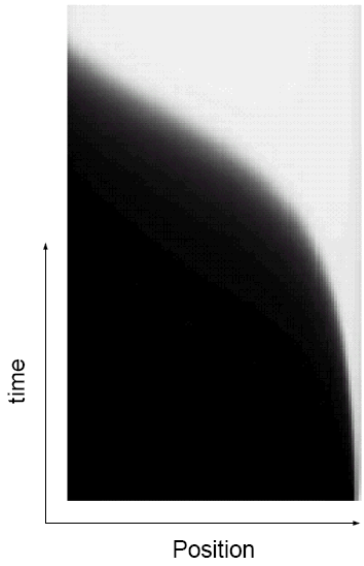

Figure 5.13. Theoretical computer simulation of local triggering [34].

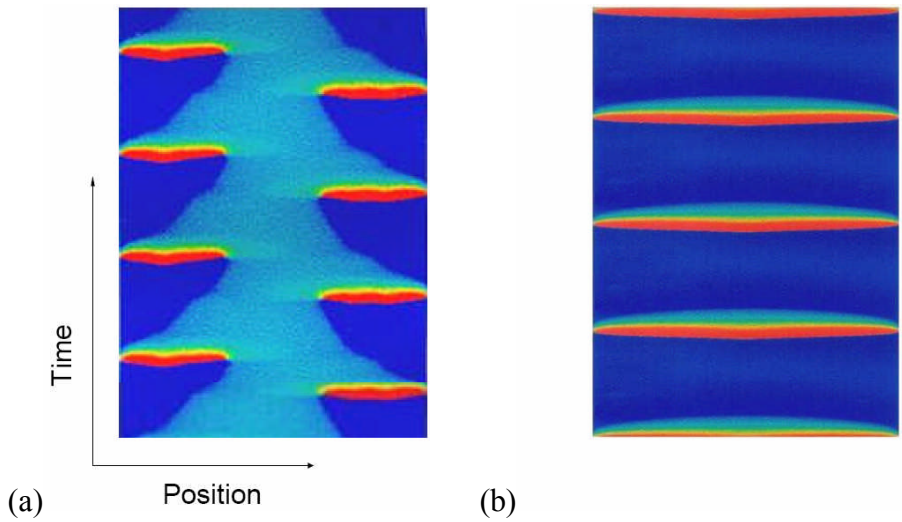

Figure 5.14. Theoretical simulations of the pattern formations of oscillations on the ribbon electrode with small β (a) and large β (b) [34].

In-phase or anti-phase pattern formation for different positions of the reference electrode (symmetric and asymmetric position) was shown in the oscillatory condition of formic acid oxidation. Anti-phase edge oscillations were observed on the anodic scan due to negative coupling with small distance between RE and WE. In-phase edge oscillations occurred when the RE was far away from the WE. Figure 5.14 shows the theoretical simulation of spatiotemporal pattern formation on a ribbon electrode with different β. In case of small β in Figure 5.14(a), the oscillations are anti-phase, similar to the experimental result in Figure 5.7(b). On the other hand, in the case of large β in Figure 5.14(b), in-phase oscillations occurred as in Figure 5.10(b).

An interesting effect occurred with the RE placed asymmetrically near one edge; there was an insertion of an extra oscillation (frequently doubling) spatially limited to the part of the ribbon closed to the RE, whereas the rest of the WE was virtually not affected.